Electronic Supplementary Information for

Liquid-phase Catalysis by Single-size Palladium Nanoclusters Supported on Strontium Titanate: Size-specific Catalysts for Suzuki-Miyaura Coupling

Hironori Tsunoyama, Haruchika Itoh, Masafumi Komori, Ryota Kobayashi,
Masahiro Shibuta, Toyoaki Eguchi, Atsushi Nakajima*

Correspondence to: nakajima@chem.keio.ac.jp

Table of Contents

Full citation of ref. 78 (S1)
Figure S1. Mass spectra for bimetallic nanocluster (NC) anions of Pd_nM_m (M = Cu and W) (S2)
Figure S2. Optimized geometries for neutral Pd_{13} NCs (S2)
Figure S3. Electrostatic potential mapping for neutral Pd_{13} NC (S3)
Figure S4. Electrostatic potential plot for neutral Pd_{13} NCs (S3)
Table S1. Coordinates for neutral Pd_{13} NC (S4)
Table S2. Charge distribution for neutral Pd_{13} NCs (S5)

Full citation of ref. 78.

M. J. Frisch, G. W. Trucks, H. B. Schlegel, G. E. Scuseria, M. A. Robb, J. R. Cheeseman, G. Scalmani, V. Barone, B. Mennucci, G. A. Petersson, H. Nakatsuji, M. Caricato, X. Li, H. P. Hratchian, A. F. Izmaylov, J. Bloino, G. Zheng, J. L. Sonnenberg, M. Hada, M. Ehara, K. Toyota, R. Fukuda, J. Hasegawa, M. Ishida, T. Nakajima, Y. Honda, O. Kitao, H. Nakai, T. Vreven, J. A. Montgomery Jr., J. E. Peralta, F. Ogliaro, M. Bearpark, J. J. Heyd, E. Brothers, K. N. Kudin, V. N. Staroverov, T. Keith, R. Kobayashi, J. Normand, K. Raghavachari, A. Rendell, J. C. Burant, S. S. Iyengar, J. Tomasi, M. Cossi, N. Rega, J. M. Millam, M. Klene, J. E. Knox, J. B. Cross, V. Bakken, C. Adamo, J. Jaramillo, R. Gomperts, R. E. Stratmann, O. Yazyev, A. J. Austin, R. Cammi, C. Pomelli, J. W. Ochterski, R. L. Martin, K. Morokuma, V. G. Zakrzewski, G. A. Voth, P. Salvador, J. J. Dannenberg, S. Dapprich, A. D. Daniels, O. Farkas, J. B. Foresman, J. V. Ortiz, J. Cioslowski and D. J. Fox, *Gaussian 09, Revision E.01; Gaussian, Inc.: Wallingford, CT*, 2013.

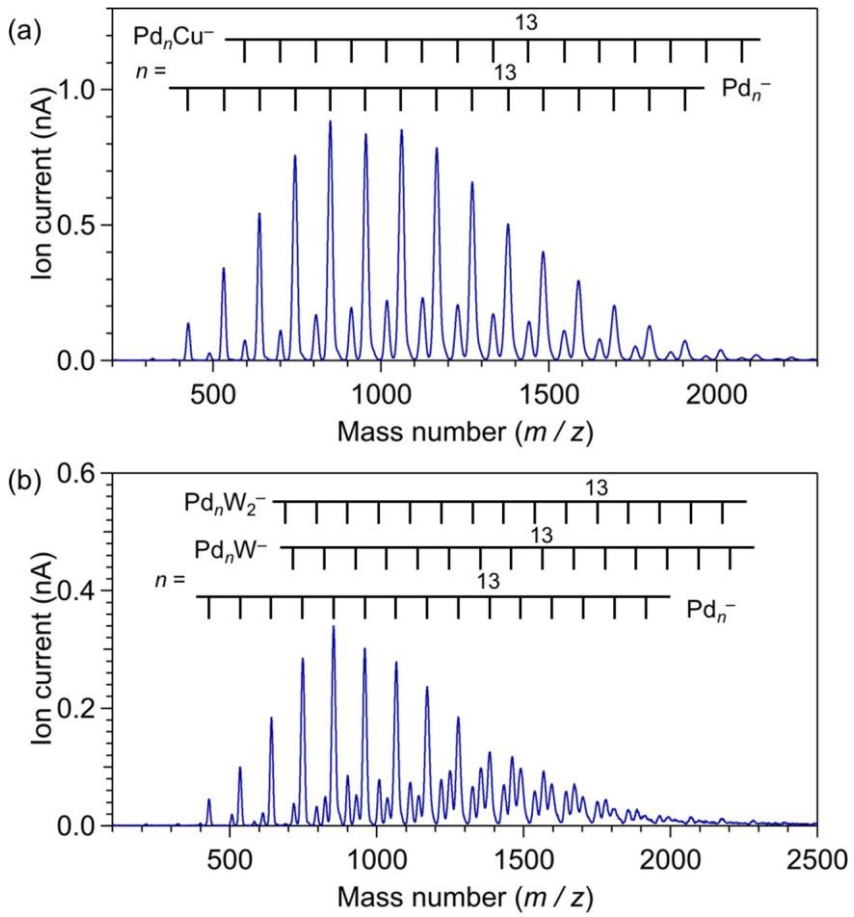

Figure S1. Mass spectra for bimetallic nanocluster (NC) anions of Pd_nM_m (M = Cu and W) produced by HiPIMS NC source. Sputtering conditions: flow rates of He and Ar are 400 and 90 sccm, respectively.

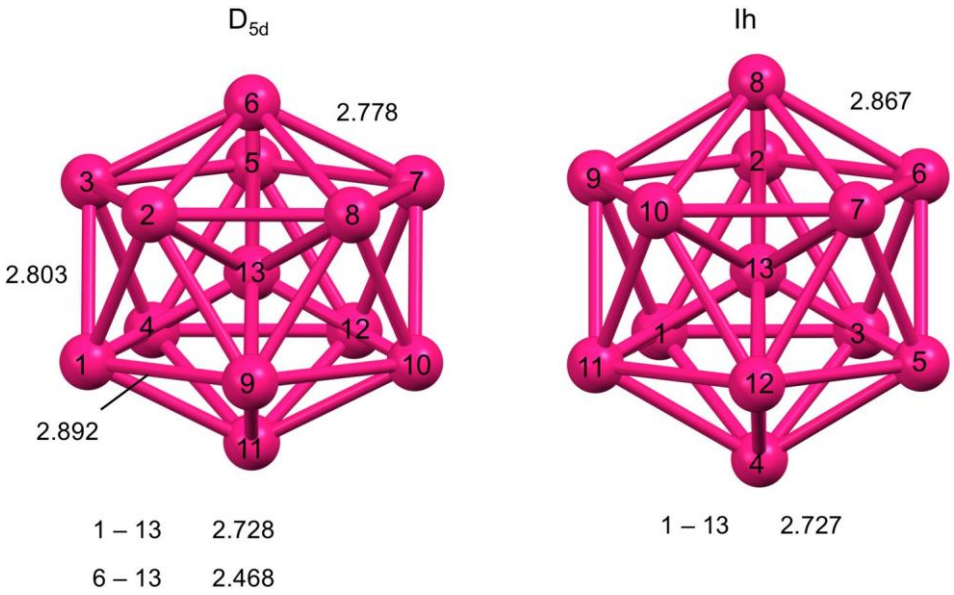

Figure S2. Optimized geometries for neutral Pd_{13} NCs with D_{5d} (most stable isomer) and I_h symmetries at PBE0/def-SV(P) level of DFT calculations, in which the former is by 0.41 eV more stable than the latter. Representative bond lengths are shown.

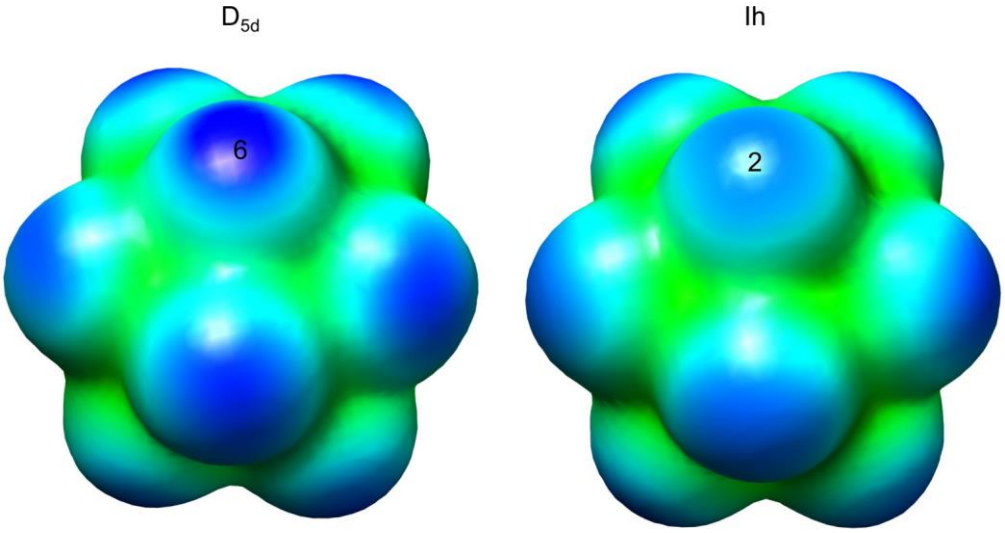

Figure S3. Electrostatic potential mapping at isoelectronic density surface of 0.010 au^{-3} for neutral Pd_{13} NCs. Deep blue color corresponds to a positive electrostatic potential.

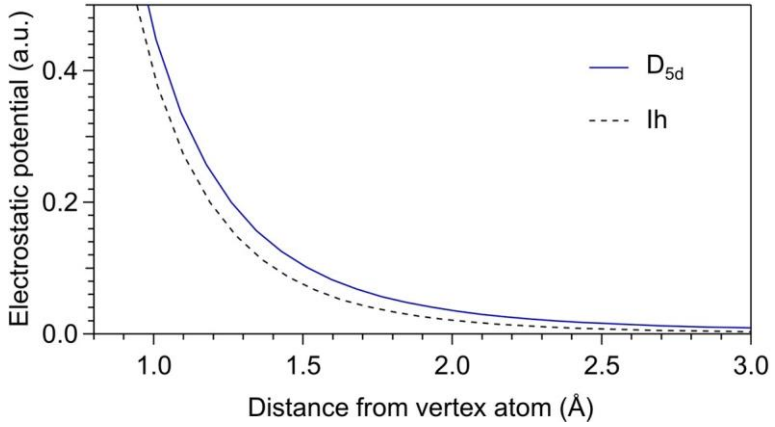

Figure S4. Electrostatic potential plot for neutral Pd_{13} NCs. Distance is defined from the center of the vertex atoms (Pd6 for D_{5d} and Pd2 for I_h isomers).

Table S1. Coordinates for neutral Pd_{13} NC optimized at PBE0/def-SV(P) level. Icosahedral isomer was optimized with symmetry constraint.

	Pd_{13} D_{5d} isomer		
	x	*y*	*z*
Pd1	0.000000	2.460315	1.177403
Pd2	1.446137	1.990437	-1.177403
Pd3	-1.446137	1.990437	-1.177403
Pd4	-2.339899	0.760279	1.177403
Pd5	-2.339899	-0.760279	-1.177403
Pd6	0.000000	0.000000	-2.467869
Pd7	0.000000	-2.460315	-1.177403
Pd8	2.339899	-0.760279	-1.177403
Pd9	2.339899	0.760279	1.177403
Pd10	1.446137	-1.990437	1.177403
Pd11	0.000000	0.000000	2.467869
Pd12	-1.446137	-1.990437	1.177403
Pd13	0.000000	0.000000	0.000000
	Pd_{13} I_h isomer		
	x	y	z
Pd1	0.000000	0.000000	2.727123
Pd2	-1.433734	-1.973365	1.219607
Pd3	1.433734	-1.973365	1.219607
Pd4	2.319830	0.753758	1.219607
Pd5	2.319830	-0.753758	-1.219607
Pd6	0.000000	-2.439213	-1.219607
Pd7	0.000000	0.000000	-2.727123
Pd8	-2.319830	-0.753758	-1.219607
Pd9	-2.319830	0.753758	1.219607
Pd10	-1.433734	1.973365	-1.219607
Pd11	0.000000	2.439213	1.219607
Pd12	1.433734	1.973365	-1.219607
Pd13	0.000000	0.000000	0.000000

Table S2. Charge distributions for neutral Pd_{13} NCs obtained by natural population analyses at PBE0/def-SV(P) level. Label for each Pd atom were shown in fig. S2.

	D_{5d} isomer		I_h isomer	
	Natural charge	Mulliken charge	Natural charge	Mulliken charge
Pd1	+0.10	+0.66	+0.12	+0.47
Pd2	+0.13	+0.59	**+0.14**	**+0.49**
Pd3	+0.13	+0.59	**+0.14**	**+0.49**
Pd4	+0.15	+0.49	+0.09	+0.47
Pd5	+0.15	+0.49	+0.09	+0.47
Pd6	**+0.16**	**+0.68**	+0.12	+0.47
Pd7	+0.10	+0.66	+0.12	+0.47
Pd8	+0.15	+0.49	+0.09	+0.47
Pd9	+0.15	+0.49	+0.09	+0.47
Pd10	+0.13	+0.59	**+0.14**	**+0.49**
Pd11	**+0.16**	**+0.68**	+0.12	+0.47
Pd12	+0.13	+0.59	**+0.14**	**+0.49**
Pd13	**-1.62**	**-7.01**	**-1.41**	**-5.71**